

Supporting information available for

**Dicationic oligotelluroxane or mononuclear telluronium cation?
Elucidation of true catalytic species and activation mechanism of
benzylic carbon-halogen bond**

Koji Takagi, Nao Sakakibara, Shoko Kikkawa, and Seiji Tsuzuki

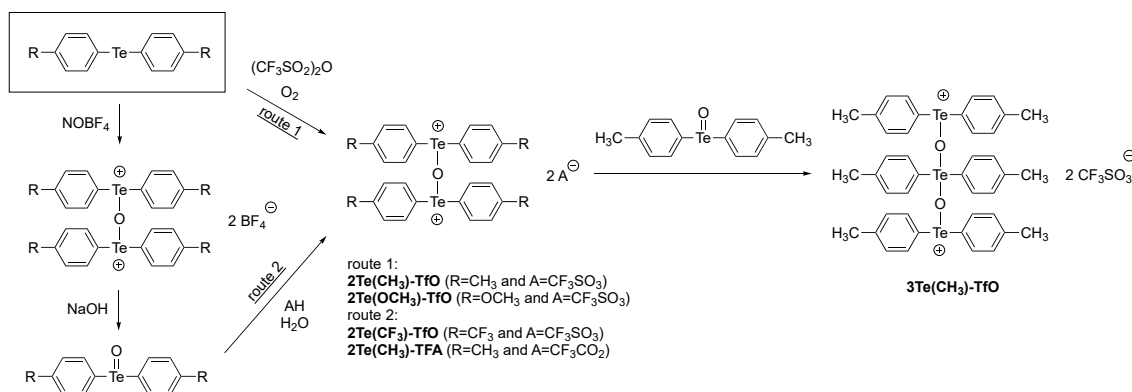
Table of contents

S1. General2
S2. Synthesis of dicationic oligotelluroxanes3
S3. Decomposition of dicationic oligotelluroxanes4
S4. Ritter-like reaction11
S5. Proof of chalcogen bonding interaction16
S6. Crystal structure analysis17
S7. Theoretical calculation20
S8. References24

S1. General

Nuclear magnetic resonance (NMR) spectroscopies were obtained on a Bruker Ascend™400 FT-NMR Spectrometer. ¹H- and ¹³C-NMR signals were referenced using a residual solvent peak as an internal standard. ¹²⁵Te-NMR signals were externally referenced to 1.0 M solution of K₂TeO₃ in D₂O (1737 ppm) against Me₂Te. Melting points (Mp) were determined on a Yanaco micro melting point apparatus MP-500D. Elemental analyses (EA) were performed on an Elementar vario EL cube in the CHN mode. All materials were obtained from commercial suppliers and used without purification unless otherwise noted. Anhydrous tetrahydrofuran (THF) and dichloromethane (DCM) were purchased from Kanto Chemical Co. Other solvents were dried and distilled following to standard methods, and stored under nitrogen atmosphere. **2Te(CH₃)-TfO**,¹ **2Te(OCH₃)-TfO**,² **2Te(CH₃)-TFA**,³ and **3Te(CH₃)-TfO**⁴ were prepared following or slightly modifying the previous reports. The purity of these compounds were completely ensured by the elemental analyses.

S2. Synthesis of dicationic oligotelluroxanes



Scheme S1. Synthetic route to dicationic oligotelluroxanes.

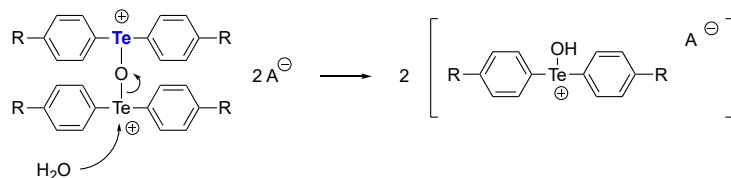
2Te(CF₃)-TfO (new compound):

CF₃SO₃H (88 μL, 1.0 mmol) was added to a MeOH solution (10 mL) of bis(4-trifluoromethylphenyl)telluroxide (216 mg, 0.50 mmol)⁵ at room temperature and the mixture was stirred for 1 h. After water (9 μL, 0.5 mmol) was added, the mixture was stirred for an additional 12 h. Solvent was removed, and the crude product was purified by recrystallization from ethyl acetate and hexane to obtain **2Te(CF₃)-TfO** in 148 mg (52% yield). m.p. 259.5-261.0 °C (decomp.); ¹H-NMR (400 MHz, CD₃CN) δ ppm 8.01 (d, J = 8.0 Hz, 4H), 7.94 (d, J = 8.0 Hz, 4H), 6.28 (s, 1H); ¹³C NMR (100 MHz, CD₃CN): δ ppm 140.5, 134.6, 134.2, 127.7, 126.0, 123.3; ¹⁹F-NMR (376 MHz, CD₃CN) δ ppm -63.84, -79.37; ¹²⁵Te-NMR (126 MHz, CD₃CN) δ ppm 1252; Elemental analysis Calcd. for C₃₀H₂₈F₆O₇S₂Te₂: C, 38.59; H, 3.02; S, 6.87; Found: C, 38.46; H, 2.98; S, 6.41.

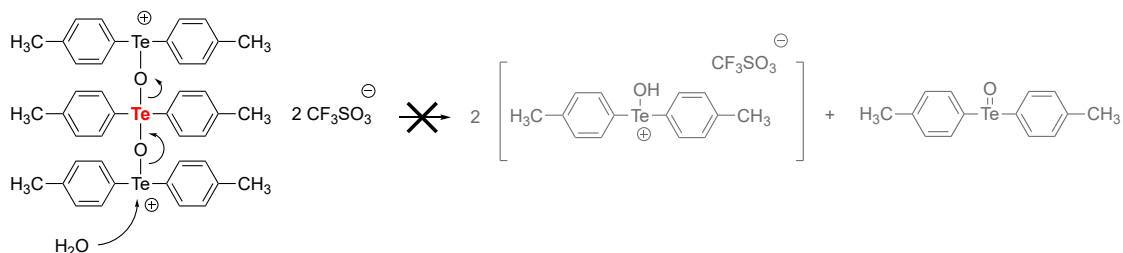
Note: Although the elemental analysis of an isolated solid product suggests the structure of **2Te(CF₃)-TfO**, the solution-state spectra likely indicate the existence of hydroxy diaryltellurium cation obtained by the decomposition of **2Te(CF₃)-TfO** (See the following section).

S3. Decomposition of dicationic oligotelluroxanes

Ditelluroxane except for **2Te(CH₃)-TFA**



Tritelluroxane



Scheme S2. Plausible decomposition mechanism. Because the cationic tellurium center of **2Te(CH₃)-TFA** is occupied by the coordination of TFA anion, the nucleophilic attack by water may be partially inhibited in contrast to the other dicationic ditelluroxanes. On the other hand, red-letter tellurium atom in **3Te(CH₃)-TfO** has a less electron-withdrawing character compared with blue-letter tellurium atom in **2Te(CH₃)-TfO**, which may result in the water-resistant property of **3Te(CH₃)-TfO**.

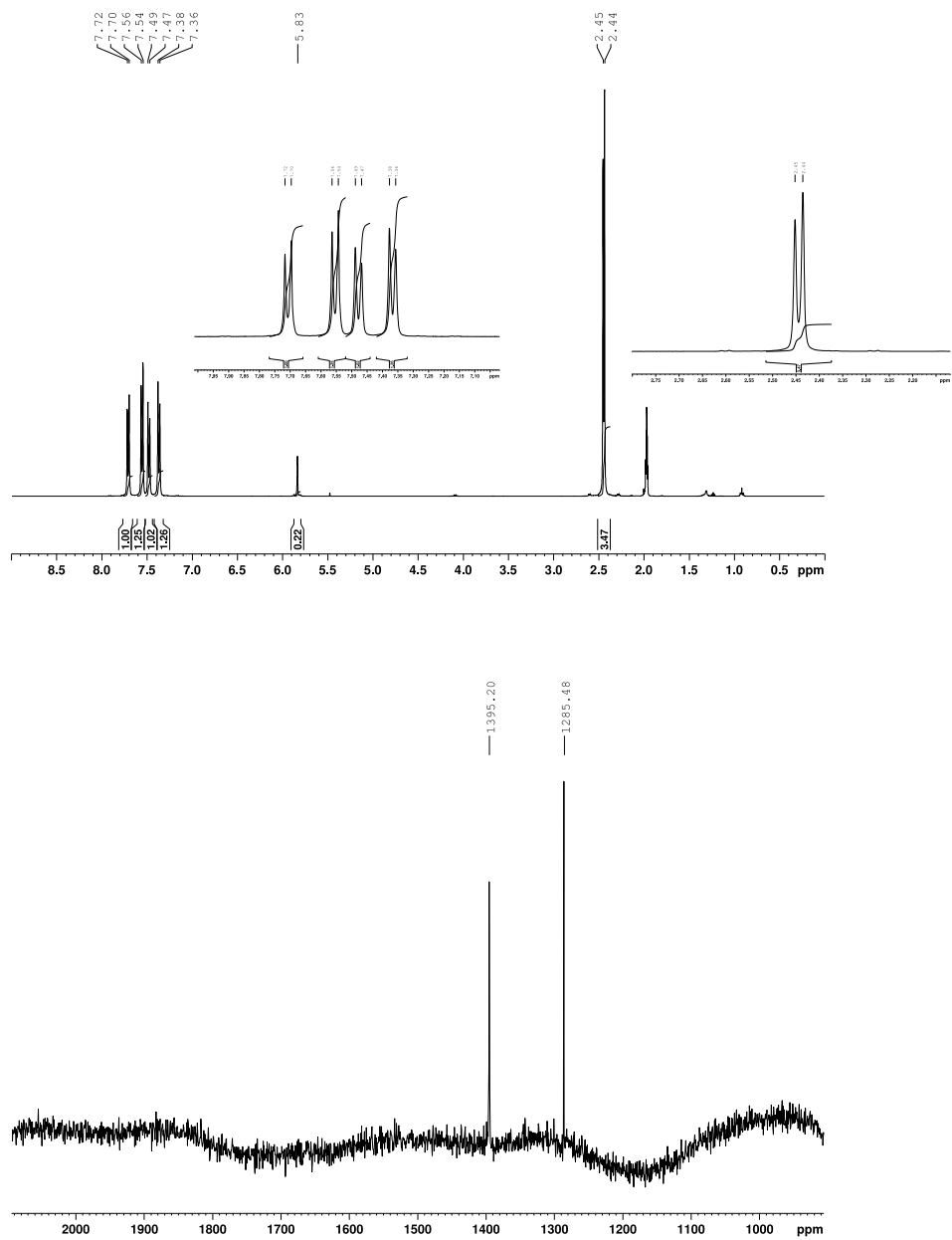


Figure S1. ^1H and ^{125}Te NMR spectra of $2\text{Te}(\text{CH}_3)\text{-TfO}$ in dried CD_3CN (containing a trace amount of water).

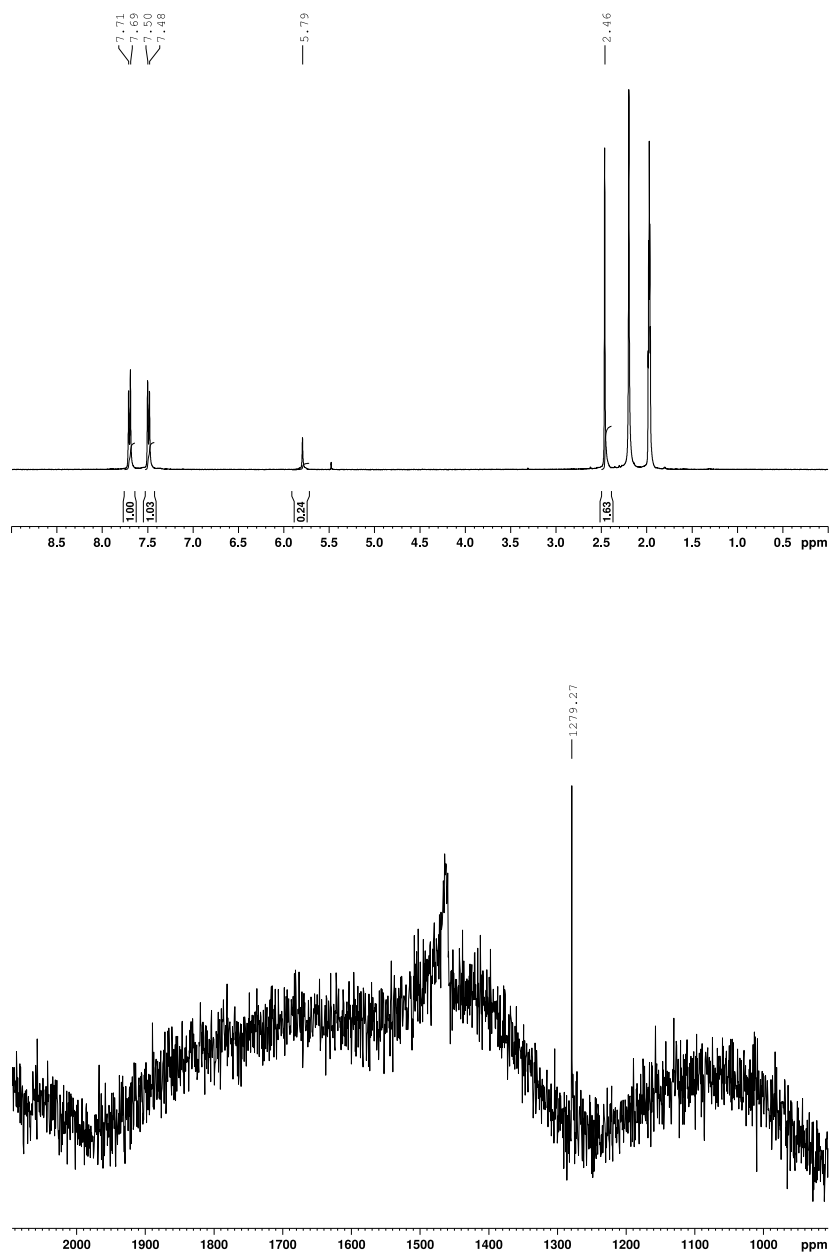


Figure S2. ^1H and ^{125}Te NMR spectra of $2\text{Te}(\text{CH}_3)\text{-TfO}$ in wet CD_3CN .

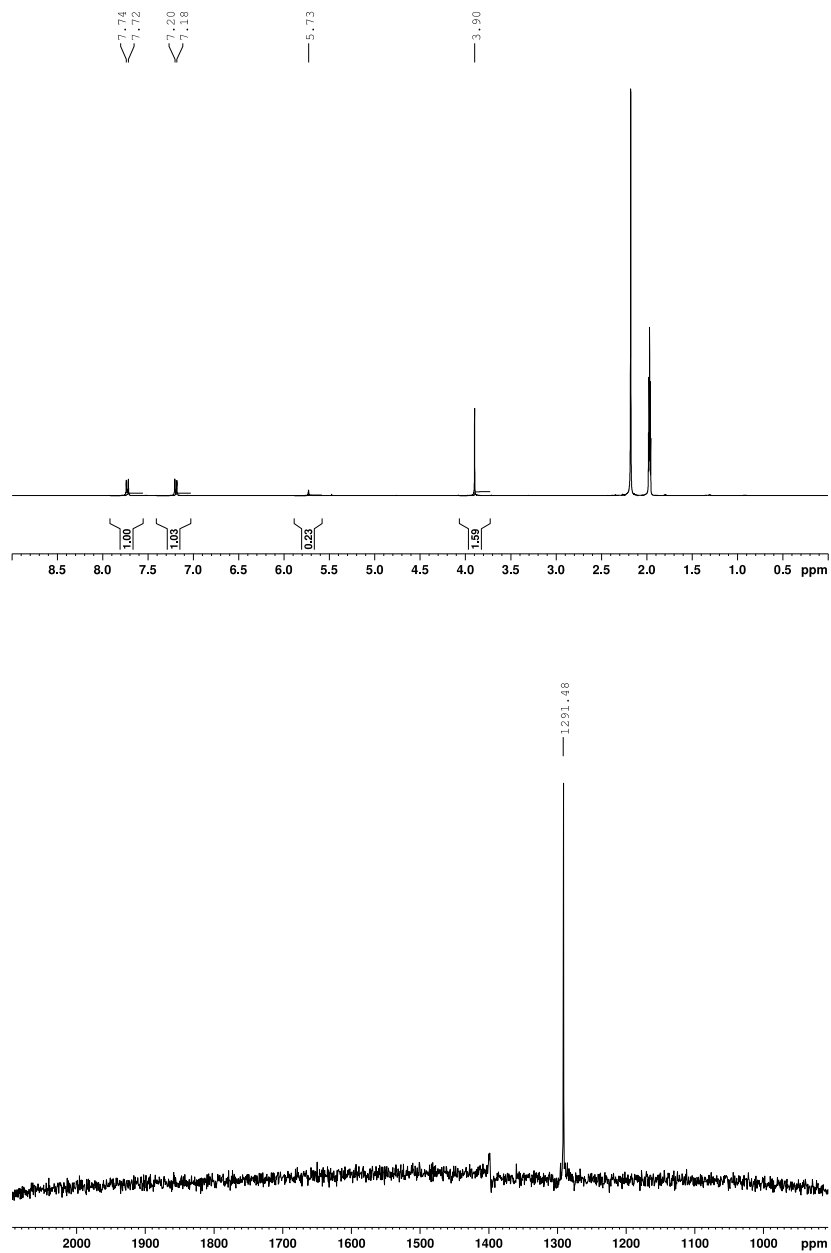


Figure S3. ¹H and ¹²⁵Te NMR spectra of 2Te(OCH₃)-TfO in wet CD₃CN.

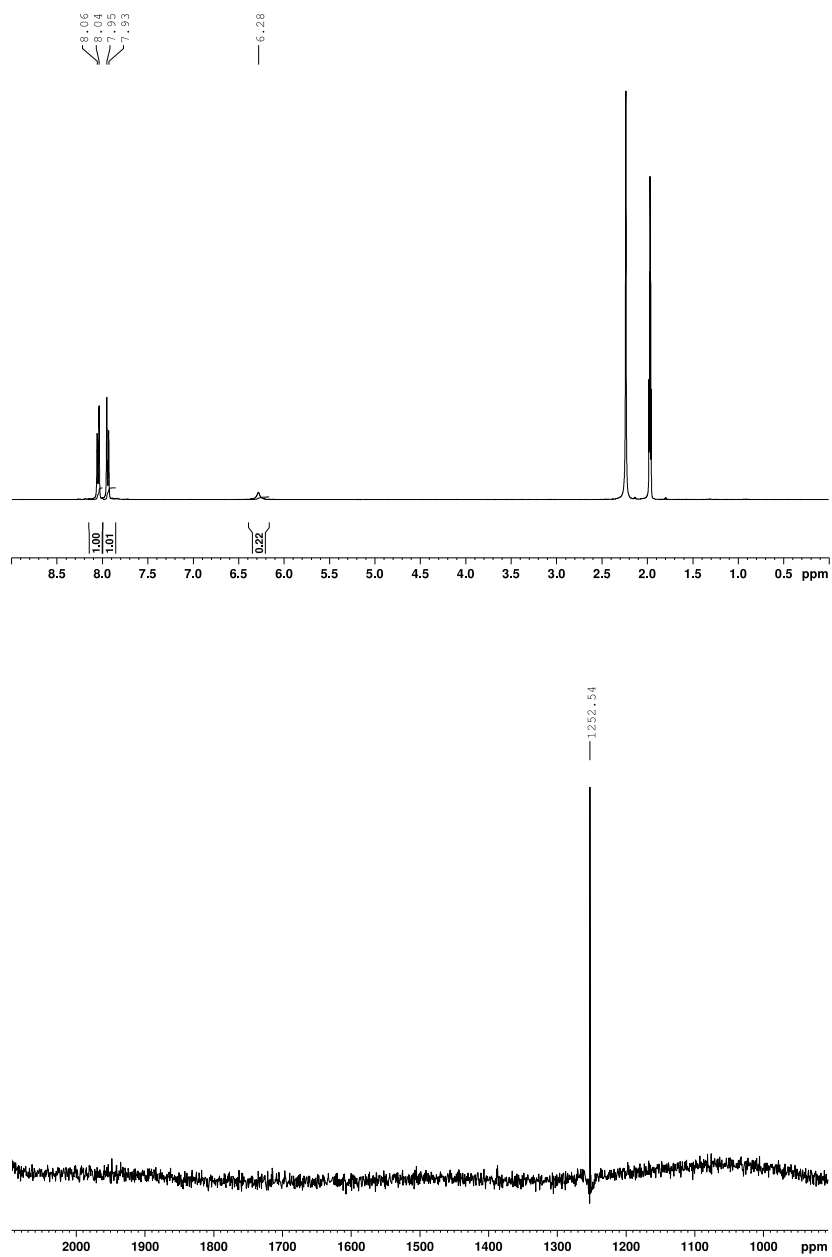


Figure S4. ^1H and ^{125}Te NMR spectra of $2\text{Te}(\text{CF}_3)\text{-TfO}$ in wet CD_3CN .

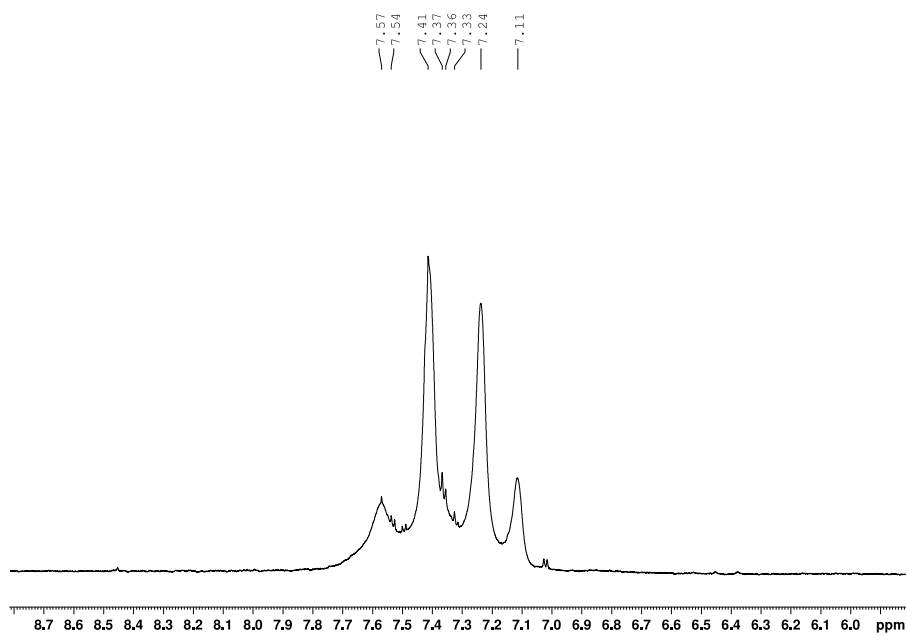
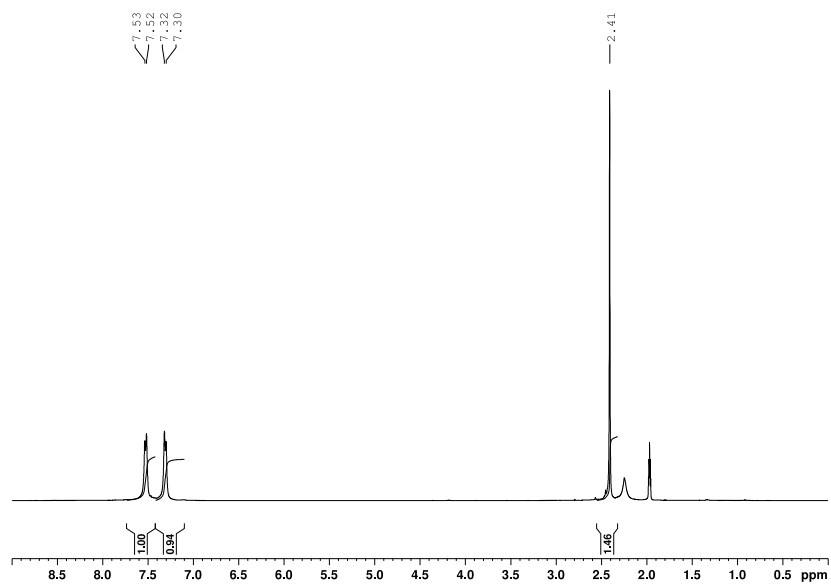


Figure S5. ^1H NMR spectrum of **3Te(CH₃)-TfO** in wet CD₃CN at 25 °C (top) and -40 °C (bottom, enlarged spectrum of aromatic region).

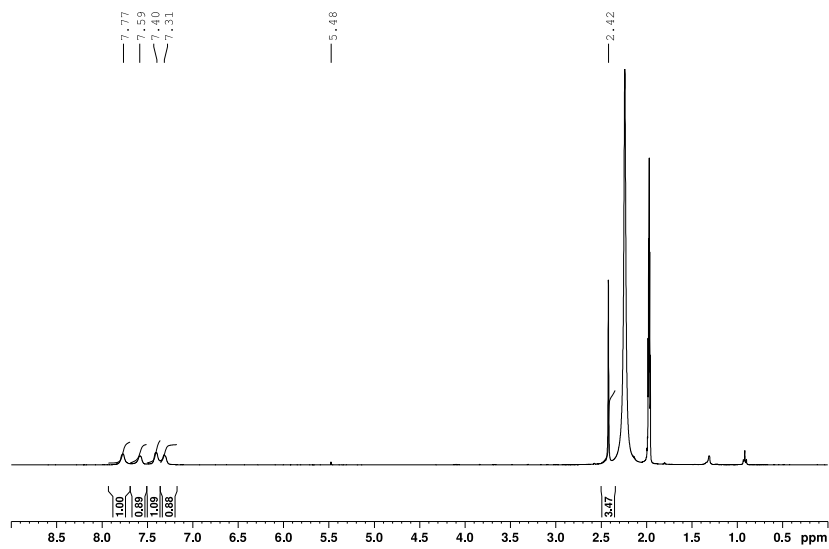
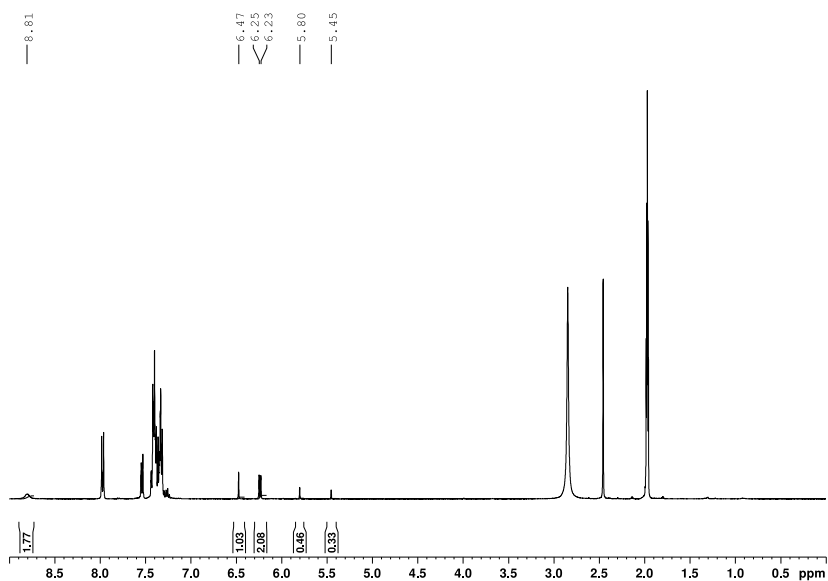
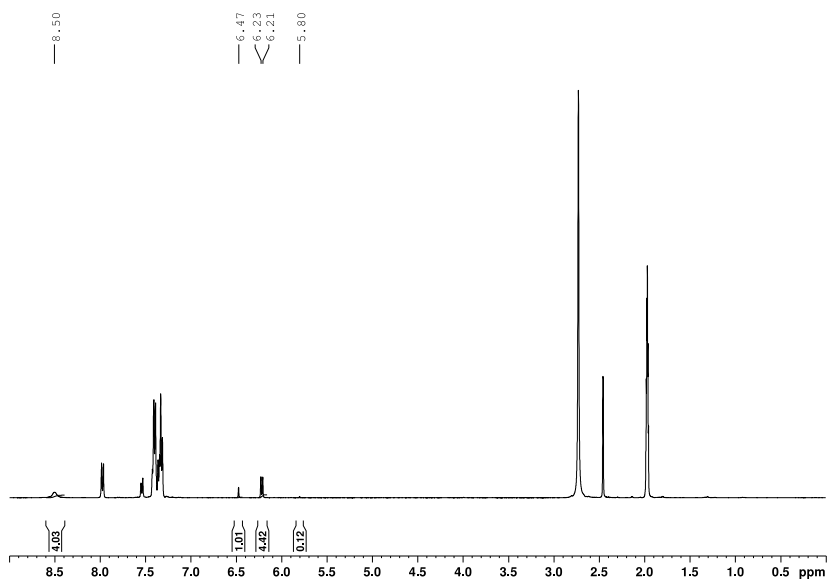


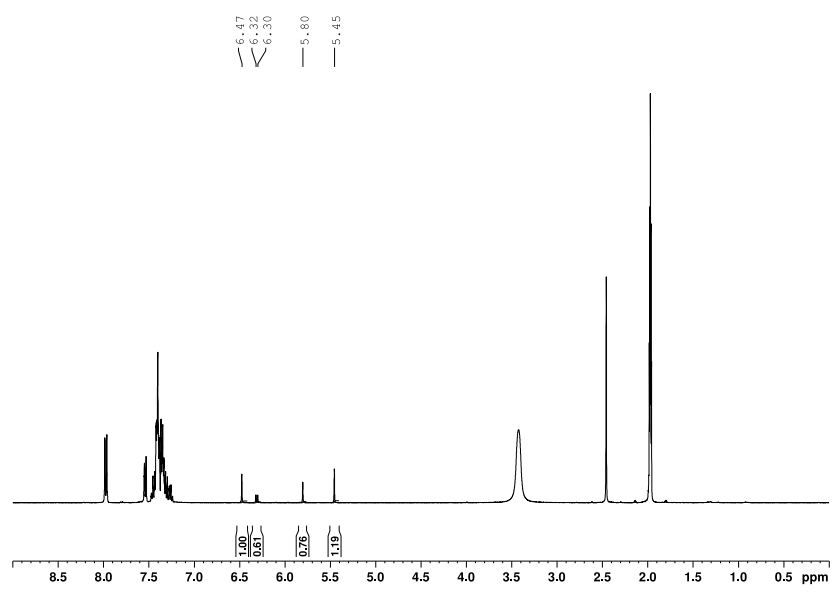
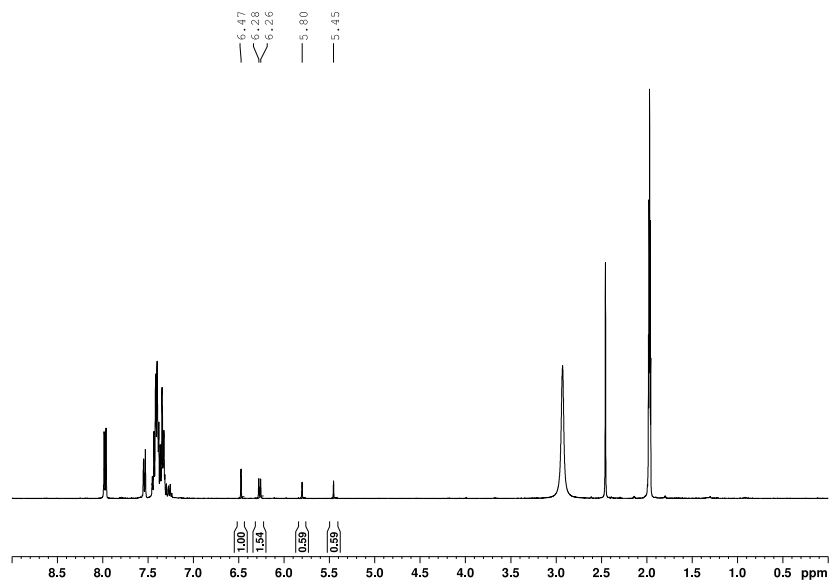
Figure S6. ^1H NMR spectrum of $2\text{Te}(\text{CH}_3)\text{-TFA}$ in wet CD_3CN .

S4. Ritter-like reaction

Preparation of stock solution: In a two-necked test tube dried by using a heating gun, bromodiphenylmethane (37 mg, 150 μmol) was dissolved in a mixture of CD_3CN (9 mL) and distilled water (8.1 mg, 3.0 equiv.). The solution was stored in a refrigerator.

Typical procedure of Ritter-like reaction: In a two-necked test tube dried by using a heating gun, organocatalyst (2 μmol) and stock solution (0.6 mL) was mixed, and the solution was transferred into a well-dried NMR tube. The NMR spectra were collected after the designated reaction time.





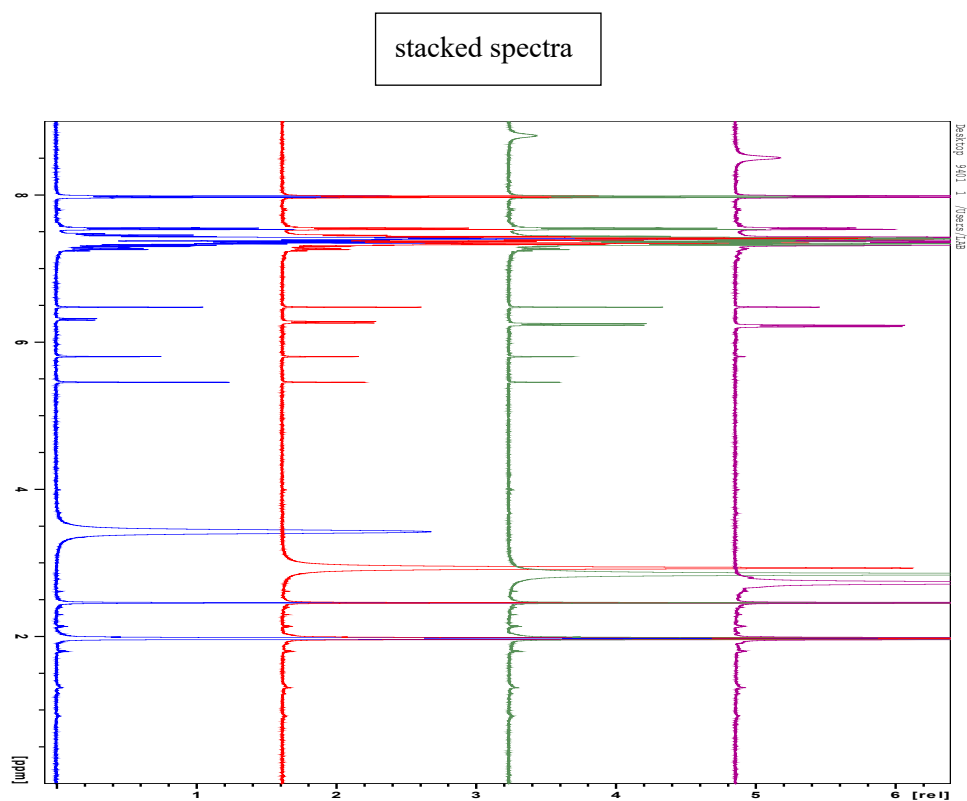


Figure S7. Selected ¹H NMR spectra in the Ritter-like reaction of bromodiphenylmethane (**1**) using **Te(CH₃)-TfO** (40 mol%) as an organocatalyst. From bottom to top: 10 min, 2 h, 8 h, and 96 h.

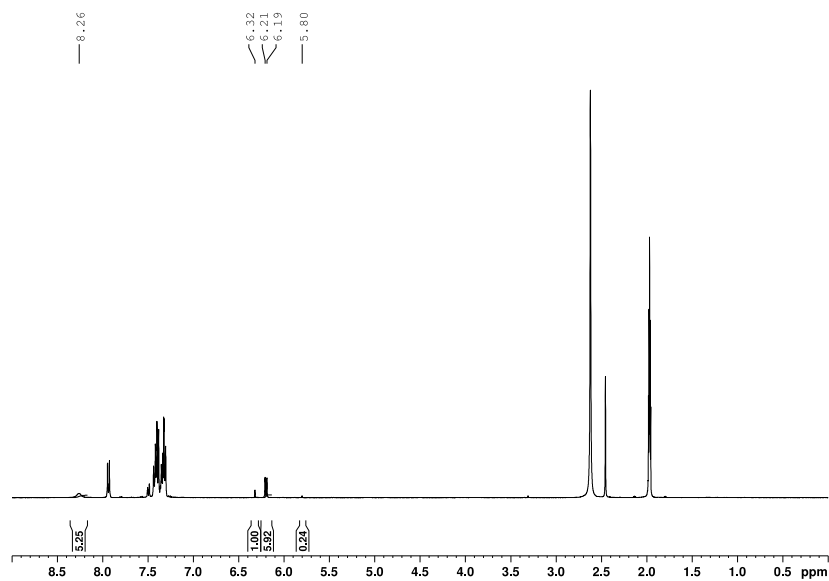


Figure S8. ^1H NMR spectrum in the Ritter-like reaction of chlorodiphenylmethane (**2**) using $\text{Te}(\text{CH}_3)\text{-TfO}$ (40 mol%) as an organocatalyst after 96 h.

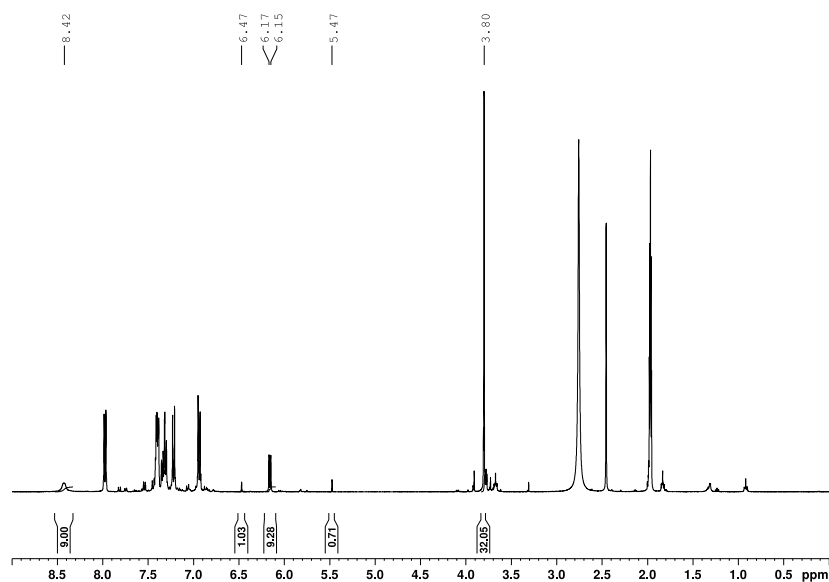


Figure S9. ^1H NMR spectrum in the Ritter-like reaction of 4-methoxy bromodiphenylmethane (**3**) using $\text{Te}(\text{CH}_3)\text{-TfO}$ (40 mol%) as an organocatalyst after 96 h.

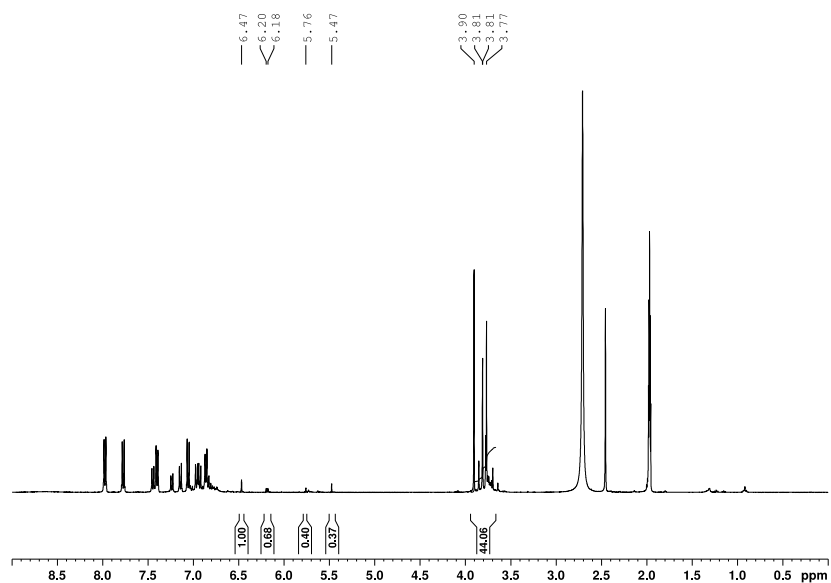


Figure S10. ^1H NMR spectrum in the Ritter-like reaction of 4,4'-dimethoxy bromodiphenylmethane (**4**) using $\text{Te}(\text{CH}_3)\text{-TfO}$ (40 mol%) as an organocatalyst after 96 h.

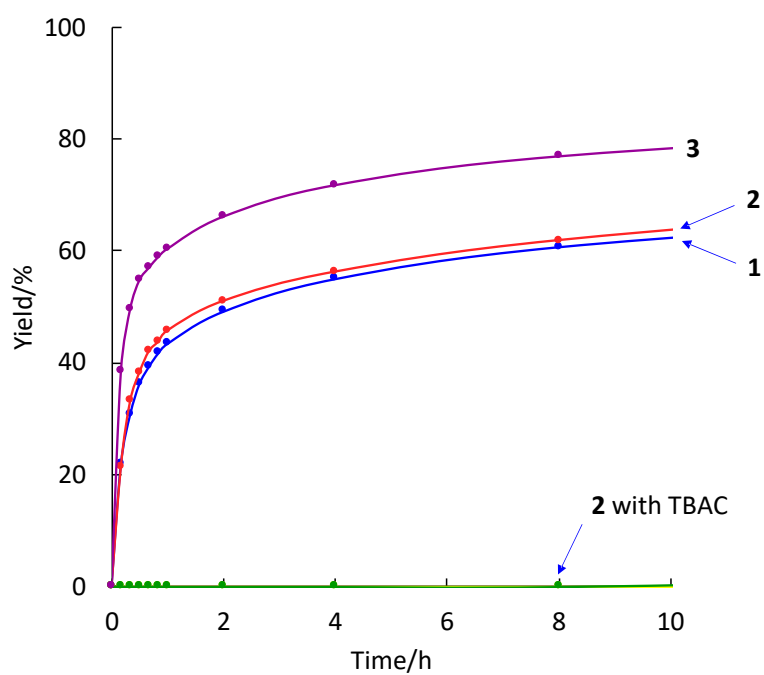


Figure S11. Plot of yield versus reaction time in the Ritter-like reaction of **1**, **2**, and **3** using $\text{Te}(\text{CH}_3)\text{-TfO}$ (40 mol%).

S5. Proof of chalcogen bonding interaction

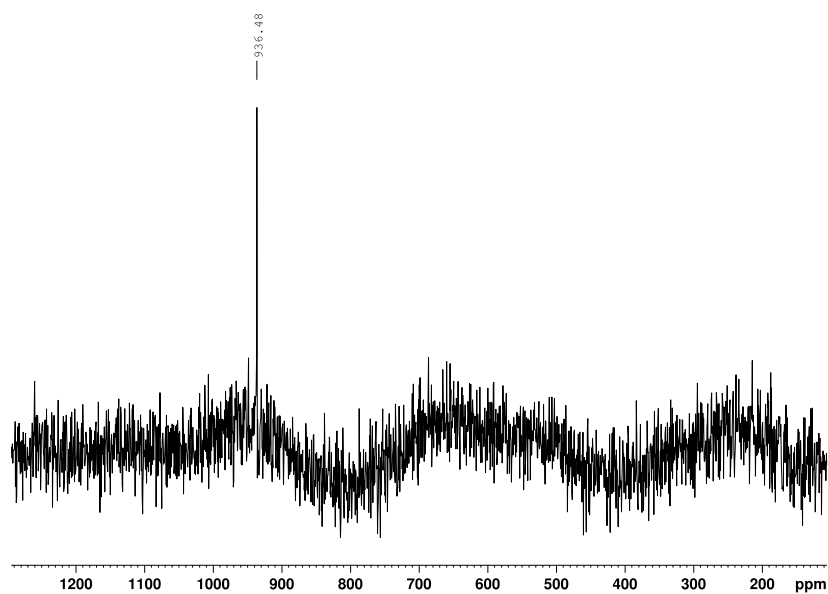


Figure S12. ^{125}Te NMR spectrum of $\text{Te}(\text{CH}_3)_2\text{O}$ in wet CD_3CN with the addition of 1 equivalent of tetra-*n*-butylammonium chloride (TBAC).

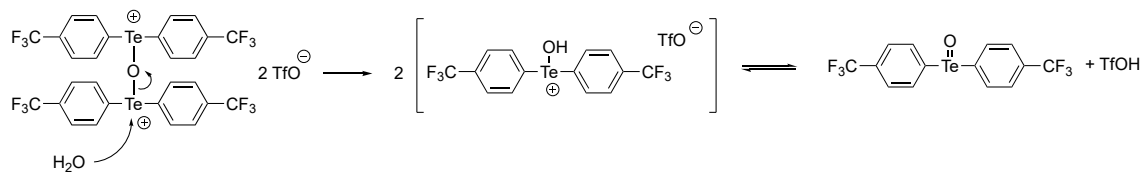
S6. Crystal structure analysis

A single crystal was mounted on a loop for the X-ray measurements. Diffraction data were collected on an X-ray diffractometer (Rigaku XtaLAB P200) equipped with a rotating-anode X-ray source (Mo $K\alpha$, $\lambda = 0.71075 \text{ \AA}$) and a hybrid photon-counting detector (PILATUS 200 K). The frame data were integrated, and absorption correction was calculated using the Rigaku CrystalClear program package. The structures were solved by SHELXT (ver. 2018/2) and refined by full-matrix least-squares fitting on F^2 (SHELXL ver. 2018/3).^{6,7} All non-hydrogen atoms were refined anisotropically and located on the calculated positions. Crystallographic data have been deposited with the Cambridge Crystallographic Data Center as supplementary publication numbers CCDC 2112083. The data can be obtained free of charge from the Cambridge Crystallographic Data Center via www.ccdc.cam. Partially occupied or highly disordered solvents located in two equivalent voids in the asymmetric unit were not modeled. Reflection contributions from these solvents were fixed and added to the calculated structure factors using the SQUEEZE function of PLATON program,⁸ which determined to be 50 electrons in 268 \AA^3 accounted for per unit cell. Because the exact identity and amount of solvents could not be identified, no solvent was included in the atom list or molecular formula. One of counter anions (containing S1 atom) was treated as ordered, and the other (containing S2, S3 atom) was treated as disordered. The latter anion had 0.5 of occupancies for each component. The CF_3 group on the benzene ring (C1–C6) bound to Te1 was treated as disordered, and it had 0.5 of occupancies for each component. The benzene ring (C8–C13) bound to Te1 was treated as disordered along with CF_3 , and they had about 0.5 of occupancies for each component. The C–C bonds of benzene ring were constrained with an AFIX 66 command. The benzene ring (C36–C41) bound to Te3 was treated as disordered along with CF_3 , and the occupancy factors of the major components were refined to be 0.60.

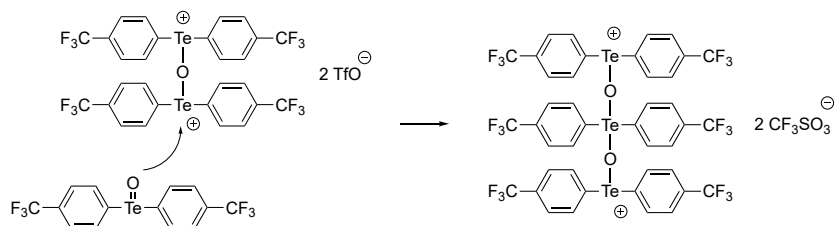
Table S1. Crystallographic parameters for the structure of **3Te(CF₃)-TfO**.

Formula	C ₄₄ H ₂₄ F ₂₄ O ₈ S ₂ Te ₃
M_r	1583.55
Crystal system	triclinic
Space group	<i>P</i> -1
$a / \text{Å}$	12.4890(3)
$b / \text{Å}$	15.9524(4)
$c / \text{Å}$	16.1392(3)
a / deg	63.246(2)
b / deg	87.5183(17)
g / deg	89.9450(19)
$V / \text{Å}^3$	2867.88(12)
Z	2
Z'	1
Temperature / <i>K</i>	93
Goodness-of-fit on F^2	1.046
$R_1 [I > 2\sigma(I)]$ on F	0.0475
wR_2 (all data) on F^2	0.1229
Reflection collected (all data)	46206
No. of reflections [$I > 2\sigma(I)$]	9365
R_{int}	0.0532
Abs. corr.	multi-scan
Radiation type	Mo $K\alpha$ ($\lambda = 0.71075 \text{ Å}$)
T_{min}	0.808
T_{max}	0.983
$2\theta_{\text{max}}$	27.499
μ / mm^{-1}	1.713

Hydrolytic decomposition



Chain extension



Scheme S3. Plausible route for producing dicationic tritelluroxane from $2\text{Te}(\text{CF}_3)\text{-TfO}$.

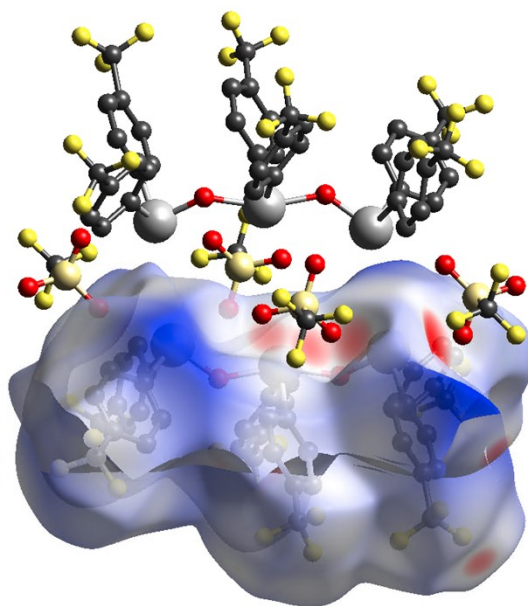


Figure S13. Three-dimensional Hirshfeld surface of a pair of $3\text{Te}(\text{CF}_3)\text{-TfO}$ molecules mapped with d_{norm} function. One can notice red areas which correspond to the ChB interaction formed between the triflate oxygen and tellurium atoms.

S7. Theoretical calculation

Density functional theory (DFT) calculations were performed using computers at Research Center for Computational Science, Okazaki, Japan. Gaussian 09 (Revision E.01)⁹ was used for the calculations. The geometries of $[(p\text{-MeC}_6\text{H}_4)_2\text{TeOH}]^+$ and its complex with substrate were optimized using the B3LYP and ωB97XD ¹⁰ functionals, respectively. The DGDZVP basis set¹¹ was used for the tellurium atom and the 6-311G(d,p) basis set was used for other atoms in the calculations. Vibrational analysis was carried out for the optimized geometries demonstrating that all the optimized geometries correspond to energy minimum structures. The interaction energy was evaluated using the ωB97XD functional with the basis set superposition error (BSSE) corrected by the counterpoise method.

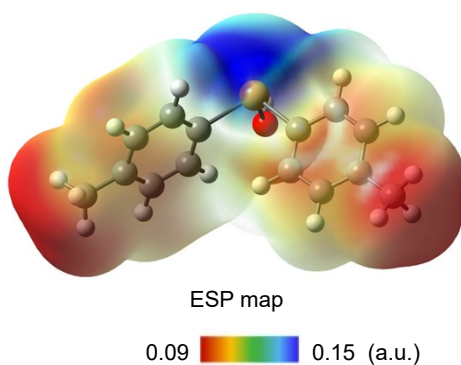


Figure S14. ESP map of $[(p\text{-MeC}_6\text{H}_4)_2\text{TeOH}]^+$.

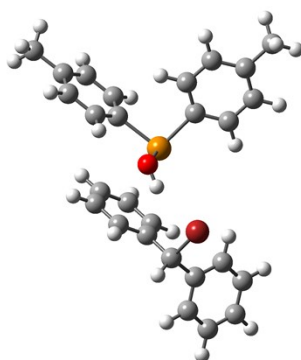


Figure S15. Optimized structure of complex.

Computational data

Optimized geometry of $[(p\text{-MeC}_6\text{H}_4)_2\text{TeOH}]^+$

C	0.1764	-0.1105	-0.0229
Te	2.0511	-0.122	0.0157
C	-0.5067	1.0194	-0.4754

C	-0.5602	-1.2127	0.4138
C	-1.9535	-1.1925	0.3867
C	-1.8999	1.0452	-0.5034
C	-2.6264	-0.0628	-0.0734
H	-0.0461	-2.1147	0.7862
H	-2.5247	-2.0707	0.7324
H	0.0524	1.9068	-0.8172
H	-2.4283	1.9436	-0.865
C	-4.1198	-0.0381	-0.1013
C	2.6872	-1.8642	-0.2642
C	2.2756	-2.5945	-1.3805
C	3.5803	-2.4536	0.6321
C	4.0513	-3.7482	0.421
C	2.743	-3.8897	-1.5962
C	3.6326	-4.4696	-0.6946
H	3.9249	-1.9006	1.5218
H	4.7563	-4.2028	1.1375
H	1.5715	-2.1516	-2.105
H	2.4086	-4.4565	-2.4816
C	4.1354	-5.8575	-0.9234
O	2.6279	0.5107	1.6557
H	3.3951	1.074	1.5317
H	5.2312	-5.8308	-1.0155
H	3.8459	-6.4885	-0.0702
H	3.6907	-6.2514	-1.8492
H	-4.4793	-0.8496	-0.7511
H	-4.4994	-0.1803	0.9213
H	-4.4546	0.9333	-0.4941

SCF Done: E(RB3LYP) = -7231.25654557 a.u.

Optimized geometry of complex

C	1.6338	-0.1299	-0.113
Te	0.0545	-1.5207	-0.2169
C	2.8963	-0.5627	-0.5382
C	1.4383	1.1715	0.3605
C	2.5263	2.0298	0.4243

C	3.9693	0.3153	-0.4667
C	3.8063	1.6203	0.0181
H	0.459	1.514	0.6706
H	2.3809	3.0394	0.7918
H	3.0508	-1.5658	-0.9202
H	4.9474	-0.0165	-0.7955
C	4.9787	2.5564	0.1201
C	-1.6392	-0.2408	-0.13
C	-2.2374	0.1599	-1.3266
C	-2.1439	0.1543	1.1082
C	-3.2622	0.9825	1.1347
C	-3.3499	0.9909	-1.2714
C	-3.8816	1.4142	-0.0452
H	-1.6856	-0.1822	2.0299
H	-3.6602	1.2952	2.0936
H	-1.8561	-0.1587	-2.2908
H	-3.8159	1.3098	-2.1969
C	-5.1089	2.2848	-0.0011
O	0.0212	-1.955	1.735
H	-0.1279	-2.902	1.8723
H	-6.0126	1.6728	-0.0909
H	-5.1761	2.8352	0.9383
H	-5.1182	3.0021	-0.8239
H	4.6766	3.5938	-0.0333
H	5.427	2.4903	1.1175
H	5.7547	2.3087	-0.6055
C	-0.4834	-5.9674	-1.8212
H	-0.1353	-6.5735	-0.9861
C	-1.9385	-6.2826	-2.0785
C	-2.4928	-6.2339	-3.3548
C	-2.751	-6.6424	-1.0023
C	-3.8366	-6.5301	-3.5484
H	-1.8724	-5.9763	-4.2046
C	-4.0914	-6.9388	-1.1951
H	-2.3281	-6.6761	-0.0032
C	-4.6393	-6.8815	-2.4719

H	-4.2552	-6.4906	-4.5476
H	-4.7103	-7.2145	-0.3489
H	-5.6871	-7.1133	-2.6254
C	0.4374	-6.1836	-2.9975
C	0.6594	-5.2216	-3.9802
C	1.034	-7.436	-3.1327
C	1.4597	-5.5097	-5.0778
H	0.2143	-4.2389	-3.8773
C	1.8349	-7.7248	-4.2298
H	0.866	-8.1945	-2.3749
C	2.0494	-6.7611	-5.2067
H	1.6276	-4.7494	-5.832
H	2.2951	-8.7024	-4.3173
H	2.6788	-6.9819	-6.0611
Br	-0.3324	-4.1241	-1.0913

SCF Done: E(RωB97XD) = -10307.3295699 a.u.

S8. References

- 1) K. Kobayashi, N. Deguchi, E. Horn and N. Furukawa, *Angew. Chem. Int. Ed.*, 1998, **37**, 984–986.
- 2) J. Beckmann, D. Dakternieks, A. Duthie, N. A. Lewcenko, C. Mitchell and M. Schürmann, *Z. Anorg. Allg. Chem.*, 2005, **631**, 1856–1862.
- 3) K. Kobayashi, K. Tanaka, H. Izawa, Y. Arai and N. Furukawa, *Chem. Eur. J.*, 2001, **7**, 4272–4279.
- 4) K. Kobayashi, N. Deguchi, O. Takahashi, K. Tanaka, E. Horn, O. Kikuchi and N. Furukawa, *Angew. Chem. Int. Ed.*, 1999, **38**, 1638–1640.
- 5) L. Engman and J. Persson, *Synth. Commun.*, 1993, **23**, 445–458.
- 6) Sheldrick, G. M. SHELXT: Integrating space group determination and structure solution. *Acta Crystallogr.* **2014**, *A70*, C1437.
- 7) Sheldrick, G. M. Crystal structure refinement with SHELXL. *Acta Crystallogr.* **2015**, *C71*, 3–8.
- 8) Spek, A. L. PLATON SQUEEZE: a tool for the calculation of the disordered solvent contribution to the calculated structure factors. *Acta Cryst. Sect. C*, **2015**, *71*, 9–18.
- 9) Gaussian 09, Revision E.01, M. J. Frisch, G. W. Trucks, H. B. Schlegel, G. E. Scuseria, M. A. Robb, J. R. Cheeseman, G. Scalmani, V. Barone, B. Mennucci, G. A. Petersson, H. Nakatsuji, M. Caricato, X. Li, H. P. Hratchian, A. F. Izmaylov, J. Bloino, G. Zheng, J. L. Sonnenberg, M. Hada, M. Ehara, K. Toyota, R. Fukuda, J. Hasegawa, M. Ishida, T. Nakajima, Y. Honda, O. Kitao, H. Nakai, T. Vreven, J. A. Montgomery, Jr., J. E. Peralta, F. Ogliaro, M. Bearpark, J. J. Heyd, E. Brothers, K. N. Kudin, V. N. Staroverov, T. Keith, R. Kobayashi, J. Normand, K. Raghavachari, A. Rendell, J. C. Burant, S. S. Iyengar, J. Tomasi, M. Cossi, N. Rega, J. M. Millam, M. Klene, J. E. Knox, J. B. Cross, V. Bakken, C. Adamo, J. Jaramillo, R. Gomperts, R. E. Stratmann, O. Yazyev, A. J. Austin, R. Cammi, C. Pomelli, J. W. Ochterski, R. L. Martin, K. Morokuma, V. G. Zakrzewski, G. A. Voth, P. Salvador, J. J. Dannenberg, S. Dapprich, A. D. Daniels, O. Farkas, J. B. Foresman, J. V. Ortiz, J. Cioslowski, and D. J. Fox, Gaussian, Inc., Wallingford CT, 2013.
- 10) J.-D. Chai and M. Head-Gordon, *Phys. Chem. Chem. Phys.* 2008, **10**, 6615–6620.
- 11) N. Godbout, D. R. Salahub, J. Andzelm and E. Wimmer, *Can. J. Chem.* 1992, **70**, 560–571.